Application of Fractional Calculus to the Modeling of Dielectric Relaxation Phenomena in Polymeric Materials

E. Reyes-Melo,[1] J. Martinez-Vega,[1] C. Guerrero-Salazar,[2] U. Ortiz-Mendez[2]

[1]*Laboratoire de Génie Electrique, Université Paul Sabatier de Toulouse (CNRS-UMR 5003), 118 Route de Narbonne, Toulouse, Cedex France*
[2]*Doctorado en Ingeniería de Materiales, Universidad Autónoma de Nuevo León, Pedro de Alba s/n, Cd. Universitaria, San Nicolás de los Garza, N.L., 66450, México*

Received 18 June 2004; accepted 29 December 2005
DOI 10.1002/app.22057
Published online in Wiley InterScience (www.interscience.wiley.com).

ABSTRACT: A model based on the concept of fractional calculus is proposed for the description of the relative complex permittivity ($\varepsilon_r^* = \varepsilon_r' - i\varepsilon_r'$, where ε_r' and ε_r'' are the real and imaginary parts of ε_r^*) in polymeric materials. This model takes into account three dielectric relaxation phenomena. The differential equations obtained for this model have derivatives of fractional order between 0 and 1. Applying the Fourier transform to fractional differential equations and considering that each relaxation mode is associated with cooperative or noncooperative movements, we have calculated $\varepsilon_r^*(i\omega,T)$ (where ω is the angular frequency and T is the temperature). The isothermal and isochronal diagrams obtained from the proposed model of ε_r' and ε_r'' clearly show three dielectric relaxation phenomena; in the isochronal case, each relaxation mode manifests by an increase in ε_r' with increasing temperature, and this behavior is associated with a peak of $\varepsilon_r''(T)$ in each case. The model is matched with the experimental data on poly(ethylene naphthalene 2,6-dicarboxylate) (PEN) to justify its validity. Poly(ethylene 2, 6–naphthalene dicarboxylate) (PEN) is a semicrystalline polymer that displays three dielectric relaxation processes: β, β^*, and α. © 2005 Wiley Periodicals, Inc. J Appl Polym Sci 98: 923–935, 2005

Key words: dielectric properties; modeling; relaxation

INTRODUCTION

Polymeric materials are often used as dielectrics in the field of electrical engineering. Their applications require a thorough knowledge of the dielectric relaxation phenomena that these materials can undergo. Dielectric relaxations are associated with molecular motions leading to a new structural equilibrium with low energy content. The process by which the polymeric macromolecules are rearranged under the application of an external electrical field is characteristic of their structure and morphology; it proceeds at a rate that increases with temperature. The morphology of these materials is an intimate mixture of crystal and amorphous phases, which give rise to a complex semicrystalline structure.[1–5] This makes an analysis of the polymer properties very difficult with the traditional calculus, and in this sense, fractional calculus is an alternative for describing the dielectric relaxations.

Correspondence to: J. Martinez-Vega (juan.martinez@lget.ups-tlse.fr).

Contract grant sponsor: ECOS (France)–ANUIES (México).
Contract grant sponsor: Universidad Autónoma de Nuevo León (Monterrey, México).

Fractional calculus is the branch of mathematics that deals with the generalization of integrals and derivatives of all real orders.[6–10] In the case of relaxation phenomena, the fractional order of a fractional integral is an indication of the remaining or preserved energy of a signal passing through a viscoelastic system (partial energy dissipation).[11] Similarly, the fractional order of a differential operator reflects the rate at which a portion of energy has been lost. In previous works, we have used fractional calculus for modeling the complex modulus in the mathematical description of three mechanical relaxations under isothermal[12,13] and isochronal conditions.[14,15] This mechanical fractional model provides a better description than the classical models formulated with integer-order derivatives.

The aim of this work is to propose a dielectric fractional model (DFM) for the description of the relative complex permittivity (ε_r^*) under isothermal and isochronal conditions, with consideration given to three relaxation phenomena. To test the validity of DFM, we have compared the model predictions and the experimental measurement data of the real (ε_r') and imaginary (ε_r'') parts of ε_r^* for a semicrystalline polymer, poly(ethylene 2,6-naphthalene dicarboxylate) (PEN). From the experimental measurements of ε_r^* for PEN,[16–19] the following relaxation modes can be observed in order of decreasing temperature: the α re-

laxation, due to the cooperative motions of chain segments by a configuration rearrangement of the entire chain, reflecting the dielectric manifestation of the glass transition; the β^* relaxation, assigned to partially cooperative molecular motions of the naphthalene groups; and the β relaxation, due to local fluctuations (noncooperative movements) of the carbonyl groups.

DIELECTRIC BEHAVIOR AND FRACTIONAL CALCULUS

Polymers are known to be electrical-insulating materials because the electrons of their atoms have very little freedom of movement. A typical model of an insulating material can be considered to be composed of small electrical dipoles. In dielectric materials, all the dipoles align (polarized) in the direction of an applied electrical field.

It must be understood that polymers are not ideal insulators. In the solid state, a semicrystalline polymer is a very good insulator, but it can become a conductor when its temperature is raised. In this case, the electrical field will give rise to charge transport.

In the domain of linearity, the electric current (I) through a material is directly proportional to the voltage (V) applied across it:

$$V = RI = RD_t^1 Q \tag{1}$$

where R is the electrical resistance and $D_t^1 Q$ is the first-order derivative of the electrical charge (Q) with respect to time.

On the other hand, an ideal insulating material can be represented by a capacitor because it does not display electrical conduction under an applied voltage. In such a case, the algebraic expression will be

$$V = \frac{Q}{C} = \frac{1}{C} D_t^0 Q \tag{2}$$

where C is the capacitance and the electrical charge can be defined as the zero-order derivative of Q with respect to time ($D_t^0 Q$).

In this way, an intermediate electrical behavior between eqs. (1) and (2) can be obtained with the fractional calculus:

$$V = \left(\frac{1}{C}\right)^{1-a} R^a D_t^a Q = \frac{(RC)^a}{C} D_t^a Q = \frac{\tau^a}{C} D_t^a Q \tag{3}$$

where $D_t^a Q$ is the fractional derivative of Q with respect to time, evidently with $a \in (0,1)$, and $RC = \tau$ is a characteristic time, called the relaxation time, that can be associated with the time required by chain segments (electrical dipoles) in movement for a complete reorganization and a full reorientation to a new state of structural equilibrium. Equation (3) represents a new electrical-fractional element named a cap resistor. From eq. (3), a resistor behavior is obtained when a is 1, and when a is 0, the electric behavior is that of a capacitor [eq. (2); see Fig. 1].

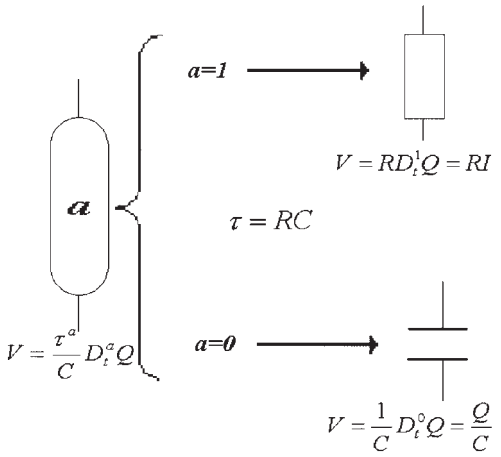

Figure 1 New electric-fractional element cap resistor.

The fractional-order derivative of Q in eq. (3) is defined as[6,11]

$$D_t^a Q(t) = D \int_0^t \frac{(t-y)^{-a}}{\Gamma(1-a)} Q(y)\, dy \; a \in (0,1) \tag{4}$$

where Γ is the gamma function:

$$\Gamma(m) = \int_0^\infty e^{-u}\, u^{m-1}\, du, \text{ with } m > 0 \tag{5}$$

Equation (4) is obtained from the Riemann–Liouville definition of a fractional-order integral. This fractional-integral operator is a generalization of noninteger values of Cauchy's formula for repeated integrations. Equation (6) is the fractional-order integral of $Q(t)$ defined between 0 and t:[6,11]

$$D_t^{-a} Q(t) = \int_0^t \frac{(t-y)^{a-1}}{\Gamma(a)} Q(y)\, dy \; a \in (0,\infty) \tag{6}$$

In the following, we are going to use the Fourier transform of a fractional differential operator, $D_t^a Q(t)$, which can be written as a product of $(i\omega)^a$ (where ω is

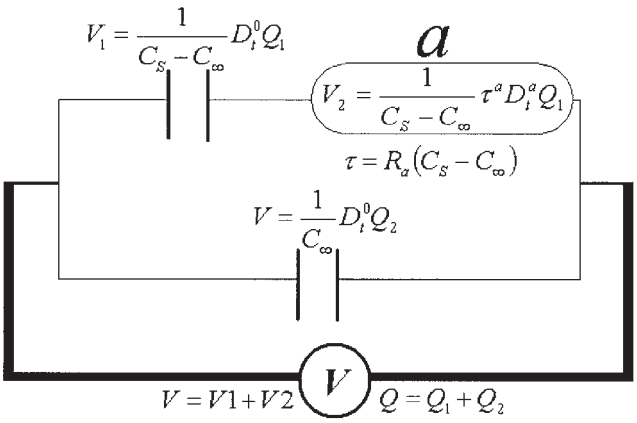

Figure 2 Electric circuit with a cap-resistor element for modeling only one dielectric relaxation phenomenon.

the angular frequency) and the Fourier transform of the function $Q(t)$.[6–10]

Using the electrical elements of Figure 1, we can build electrical circuits for modeling ε_r^* of polymeric materials. In dynamic dielectric spectrometry, a sinusoidal alternating voltage (V) of very low amplitude having an angular frequency (ω) is applied to a polymer specimen inducing an electric current (I). V and I are out of phase at an angle $0 < \theta < \pi/2$; consequently, V, I, and the admittance (Y; the inverse of impedance) can be written as complex numbers in the following way:

$$V^* = V_0 \exp(i\omega t)\ I^* = I_0 \exp(i\omega t + \theta)\ Y^* = \frac{I^*}{V^*} \quad (7)$$

From admittance Y^*, using eq. (8), we can estimate to a first approximation the complex capacity (C^*) or ε_r^*:

$$\varepsilon_r^* = \frac{\varepsilon^*}{\varepsilon_0} = \frac{C^*}{C_0} = \frac{Y^*}{i\omega C_0} \quad (8)$$

where ε^* is the absolute complex permittivity of the polymer and ε_0 and C_0 are the permittivity and the capacitance of free space, respectively.

Figure 2 is an electrical circuit obtained by the substitution of R by a cap resistor in the classical Debye model. This new fractional model is analogous to the fractional Zener model[9,12–15] used for the mathematical description of the complex elastic modulus characterized by only one relaxation phenomenon.

The fractional differential equation obtained for this electrical circuit is

$$V = \frac{Q - C_\infty V}{C_S - C_\infty} + \frac{\tau^a}{C_S - C_\infty} D_t^a (Q - C_\infty V) \quad (9)$$

where V is the applied voltage, C_S is the capacitance at a low frequency (or high temperature), C_∞ is the capacitance at a high frequency (or low temperature), and τ is the characteristic time of the electric circuit in Figure 2. Equation (9) provides us, after Fourier transformation, ε_r' and ε_r'':

$$\varepsilon_r' = \varepsilon_{r\infty} + \frac{(\varepsilon_{rs} - \varepsilon_{r\infty})\left[1 + [\omega\tau]^a \cos\left(a\frac{\pi}{2}\right)\right]}{\left[1 + [\omega\tau]^a \cos\left(a\frac{\pi}{2}\right)\right]^2 + \left[[\omega\tau]^a \sin\left(a\frac{\pi}{2}\right)\right]}$$

$$\varepsilon_r'' = \frac{(\varepsilon_{rs} - \varepsilon_{r\infty})\left[[\omega\tau]^a \sin\left(a\frac{\pi}{2}\right)\right]}{\left[1 + [\omega\tau]^a \cos\left(a\frac{\pi}{2}\right)\right]^2 + \left[[\omega\tau]^a \sin\left(a\frac{\pi}{2}\right)\right]} \quad (10)$$

where ε_{rs} is the relative permittivity at a low frequency (or high temperature) and $\varepsilon_{r\infty}$ is the relative permittivity at a high frequency (or low temperature). The τ parameter is associated with the relaxation time of molecular motions of the dielectric relaxation phenomenon. In polymers, the relaxation time is temperature-dependent and under isothermal conditions can be assumed to be constant; consequently, eq. (10) depends on the frequency and parameter a. The values of $\varepsilon_r'(\omega)$ and $\varepsilon_r''(\omega)$ can be combined in a single curve called a Cole–Cole diagram. Figure 3 shows Cole–Cole diagrams obtained from eq. (10) at different values of parameter a. A qualitative classical dielectric response for polymers can be obtained with values of a between 0 and 1. These diagrams are symmetrical at all values of parameter a; however, it is well known that for polymers in a glassy state, the Cole–Cole diagrams are asymmetrical curves.[20–22]

To obtain the asymmetrical behavior in the Cole–Cole diagrams, it is necessary to add a second cap resistor, b, to the model of Figure 2 (see Fig. 4). This model is characterized by two mechanisms. The first cap-resistor element, a, characterizes short times, τ_a, associated with the electrical behavior in the high-frequency or low-temperature region. The second cap resistor, b, characterizes long times, τ_b, associated with the electrical behavior in the low-frequency or high-temperature region.

The fractional differential equation obtained for this model is

$$Q = C_\infty V + (C_S - C_\infty)\left[\tau_a^{-a} D_t^{-a}\left(V - \frac{Q - C_\infty V}{C_S - C_\infty}\right) + \tau_b^{-b} D_t^{-b}\left(V - \frac{Q - C_\infty V}{C_S - C_\infty}\right)\right] \quad (11)$$

Applying the Fourier transformation to eq. (11) and using eq. (8), we obtain ε_r' and ε_r'':

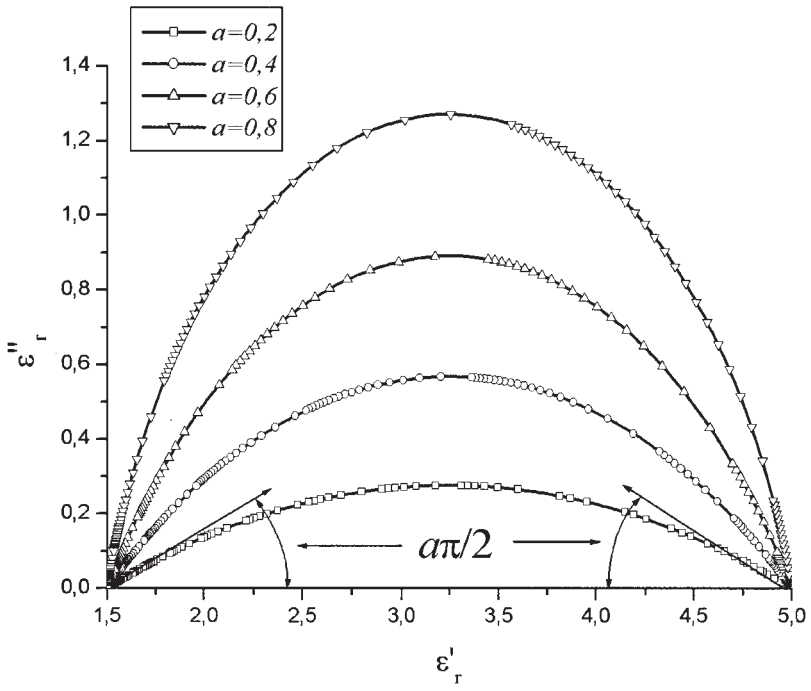

Figure 3 Cole–Cole diagrams under isothermal conditions obtained from eq. (10), with $\tau = 100$ s, $\varepsilon_{rs} = 5$, and $\varepsilon_{r\infty} = 1.5$.

$$\varepsilon_r' = \varepsilon_{rs} - \frac{(\varepsilon_{rs} - \varepsilon_{r\infty 1})\left[1 + [\omega\tau_b]^{-b}\cos\left(b\frac{\pi}{2}\right) + [\omega\tau_a]^{-a}\cos\left(a\frac{\pi}{2}\right)\right]}{\left[1 + [\omega\tau_b]^{-b}\cos\left(b\frac{\pi}{2}\right) + [\omega\tau_a]^{-a}\cos\left(a\frac{\pi}{2}\right)\right]^2 + \left[[\omega\tau_b]^{-b}\sin\left(b\frac{\pi}{2}\right) + [\omega\tau_a]^{-a}\sin\left(a\frac{\pi}{2}\right)\right]^2}$$

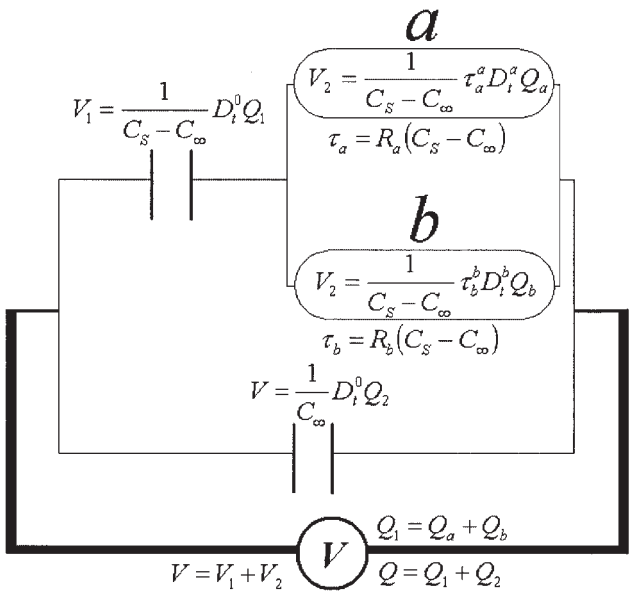

Figure 4 Electric circuit with two cap resistors for modeling only one dielectric relaxation phenomenon in polymeric materials.

$$\varepsilon_r'' = \frac{(\varepsilon_{rs} - \varepsilon_{r\infty 1})\left[[\omega\tau_b]^{-b}\sin\left(b\frac{\pi}{2}\right) + [\omega\tau_a]^{-a}\sin\left(a\frac{\pi}{2}\right)\right]}{\left[1 + [\omega\tau_b]^{-b}\cos\left(b\frac{\pi}{2}\right) + [\omega\tau_a]^{-a}\cos\left(a\frac{\pi}{2}\right)\right]^2 + \left[[\omega\tau_b]^{-b}\sin\left(b\frac{\pi}{2}\right) + [\omega\tau_a]^{-a}\sin\left(a\frac{\pi}{2}\right)\right]^2} \quad (12)$$

Figure 5 shows the classical asymmetrical response (Cole–Cole diagrams) of the system [eq. (12)] under isothermal conditions. The maximum of ε_r'' obtained is associated with one relaxation phenomenon. In Figure 5, we confirm the fact that two cap resistors can reproduce the different dielectric behaviors of the system at low and high frequencies. The slope at low values of ε_r' (low temperature or high frequency) will be $a\pi/2$, and in the region of high values of ε_r' (high temperature or low frequency), this angle will be $b\pi/2$.

The model of Figure 4, even with two cap resistors, can represent only the dielectric behavior of polymers in the neighborhood of one relaxation phenomenon. This model cannot be used for polymers with three distinct dielectric relaxations. In such a case, the Cole–Cole diagrams must show three distinct peaks.

We present, therefore, another fractional model with the aim of predicting the dielectric behavior of polymers with three relaxation phenomena (α, β^*, and β for PEN). We have developed a DFM based on three electrical circuits arranged in parallel (see Fig. 6). The first one possesses two cap resistors, *a* and *b*, and is

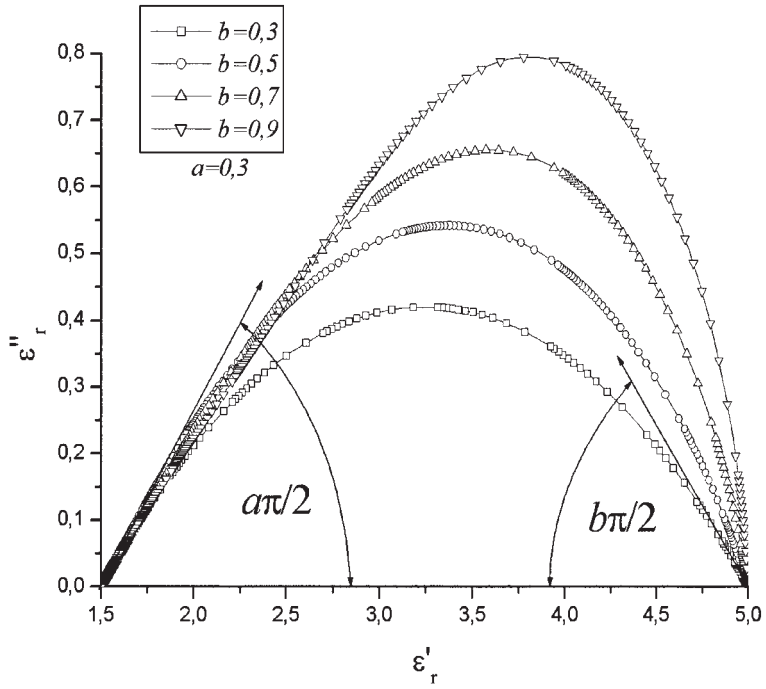

Figure 5 Cole–Cole diagram obtained under isothermal conditions from eq. (12), with $\tau_a = 100$ s, $\tau_b = 110$ s, $\varepsilon_{rs} = 5$, and $\varepsilon_{r\infty} = 1.5$.

mainly associated with the α relaxation. The second one has only one cap resistor, c, and is associated with the β^* relaxation. The last one also has only one cap resistor, d, and is associated with the β relaxation.

In the DFM, the electric charge is the result of the contributions of elements 1, 2, and 3:

$$Q = Q1 + Q2 + Q3 \tag{13}$$

V is equal to the individual voltage of each element:

$$V = V1 = V2 = V3 \tag{14}$$

Applying the Fourier transformation to eq. (13) and using eqs. (14) and (8), we find that ε_r^* can be expressed as a function of the relative complex permittivities of each element of our DFM:

$$\varepsilon_r^* = \varepsilon 1_r^* + \varepsilon 2_r^* + \varepsilon 3_r^* = \varepsilon_r' - i\varepsilon_r'' \tag{15}$$

$$\varepsilon_r' = \varepsilon 1_r' + \varepsilon 2_r' + \varepsilon 3_r' \tag{16}$$

$$\varepsilon_r'' = \varepsilon 1_r'' + \varepsilon 2_r'' + \varepsilon 3_r''' \tag{17}$$

In eqs. (16) and (17), $\varepsilon 1_r'$ and $\varepsilon 1_r''$ are the same, already defined by eq. (12). For element 2 of Figure 6, related to β^* relaxation, $\varepsilon 2_r'$ and $\varepsilon 2_r''$ are the same as those in eq. (10), and third element is equivalent to the second one, with $\varepsilon 3_r'$ and $\varepsilon 3_r''$ also defined by eq. (10).

Figure 7 presents Cole–Cole diagrams obtained under isothermal conditions from eqs. (16) and (17). In this case, we have verified the behavior of DFM at different values of b; the remaining parameters, a, c, and d, are constants.

Figure 7 shows how our model predicts the existence of three maxima corresponding to dielectric relaxations: β; β^*; and α. The maximum at lower values of ε_r' represents the β relaxation, the second maximum is associated with the β^* relaxation, and the last one at higher values of ε_r' is associated with the α relaxation. However, parameters a and b are associated mainly with the α relaxation, c is associated with β^*, and d is associated with β.

The Cole–Cole diagrams of Figure 7 were obtained from the frequency dependence of the real and imaginary parts of ε^*. However, in practice, it is very useful to study and analyze the temperature dependence of ε^* (isochronal conditions). The isochronal spectra of ε_r' and ε_r'' can be obtained from eqs. (16) and (17) because of the temperature dependence of the parameters: τ_a, τ_b, τ_c, and τ_d.

ISOCHRONAL BEHAVIOR OF ε_r^*

To obtain the temperature dependence of ε_{rr}^* we need to define the relationship between the relaxation time, τ, and the temperature, T, which in turn depends on the cooperative and noncooperative nature of the molecular motions[23,24] associated with each dielectric re-

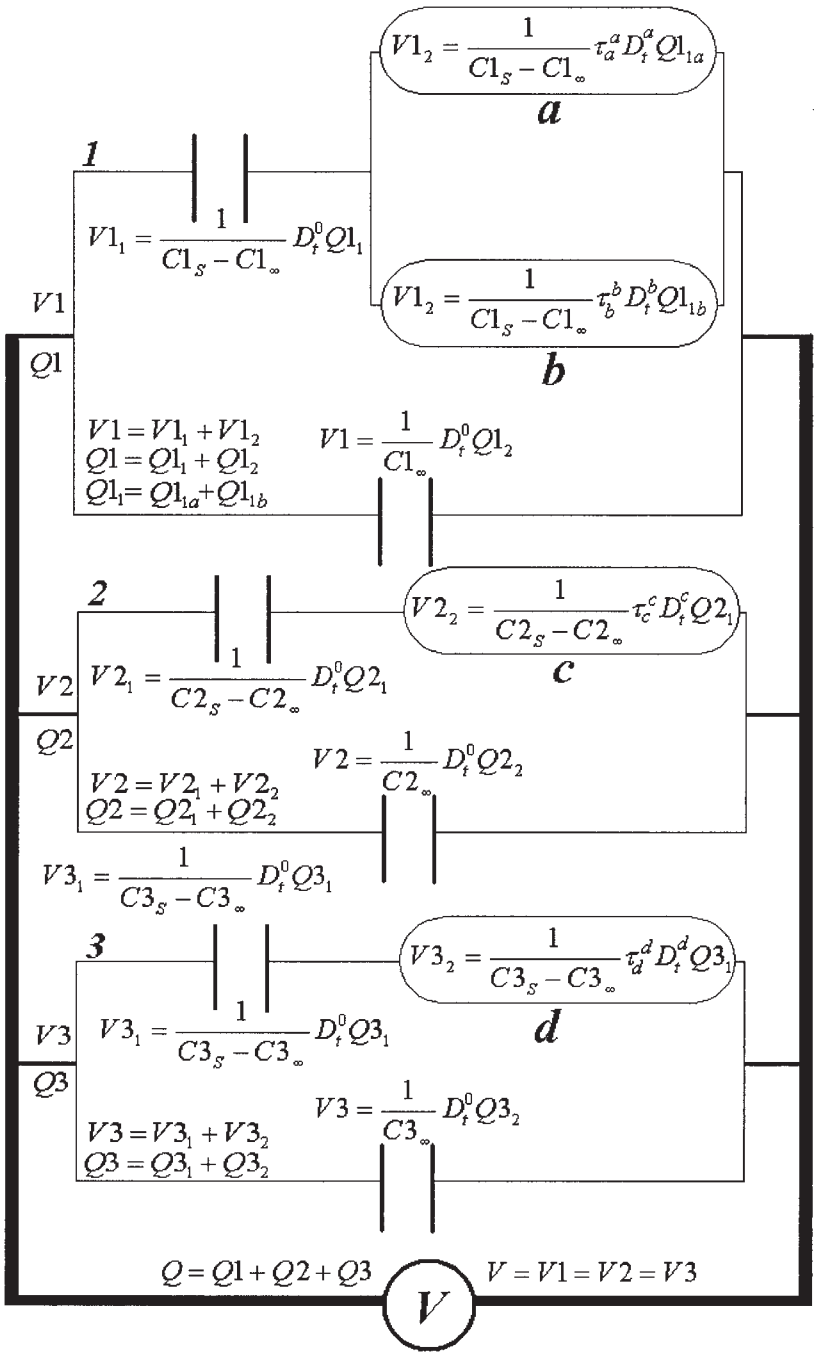

Figure 6 DFM for α, β^*, and β dielectric relaxations of PEN.

laxation phenomenon. The cooperative movements are simultaneous motions of macromolecular chain segments due to the interference with the neighboring chain segments. In a noncooperative process, the chain segments are able to move without any interference with their neighbors, being much localized movements.

$\tau(T)$, for noncooperative motions follows an Arrhenius law behavior:

$$\tau(T) = \tau_0 \exp\left(\frac{E_a}{k_B T}\right) \tag{18}$$

where the activation energy (E_a) could have magnitudes identifiable with real energy barriers;[25] k_B is the Boltzmann constant; T is the absolute temperature; and τ_0 is the pre-exponential factor, falling typically within the range of 10^{-16} s $\leq \tau_0 \leq 10^{-13}$ s. The values of τ_0 in the vicinity of the upper limit correspond to molecular vibrational times, and the lower limit may be rationalized by an additional entropy contribution.[25] In the case of PEN, several works have shown that the relaxation times of the β relaxation obey the Arrhenius law.[16–19]

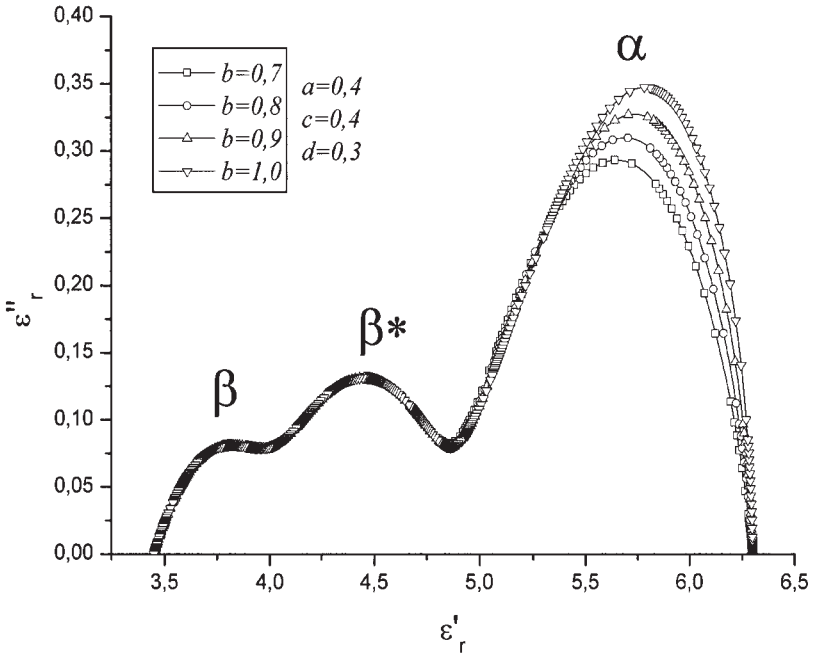

Figure 7 Cole–Cole diagram obtained from the model of Figure 4 under isothermal conditions, with $\tau_a = 100$ s, $\tau_b = 200$ s, $\tau_c = 1 \times 10^{-4}$ s, $\tau_d = 1 \times 10^{-9}$ s, $\varepsilon 1_{rs} = 2.5$, $\varepsilon 1_{r\infty} = 1.1$, $\varepsilon 2_{rs} = 2$, $\varepsilon 2_{r\infty} = 1.15$, $\varepsilon 3_{rs} = 1.8$, and $\varepsilon 3_{r\infty} = 1.2$.

On the other hand, for a cooperative process, the probability of success of cooperative motions is P^Z, with $P \propto 1/\tau$ representing the probability of a single elementary movement, and exponent Z can be considered the number of elementary movements. Consequently, $\tau_{\text{cooperative}}$ represents a power law in a temperature range from T_0 to the crossover temperature (T^*):[24]

$$\tau_{\text{cooperative}}(T) = \tau_0\left(\frac{\tau}{\tau_0}\right)^Z = \tau_0\left[\exp\left(\frac{E_{\text{a elementary movements}}}{k_B T}\right)\right]^Z \quad T_0 \leq T \leq T^* \quad (19)$$

In eq. (19), τ is the relaxation time of the elementary movement defined by an Arrhenius behavior, and Z is dependent on the polymer structure and is determined from the next equation:[23,24]

$$Z(T) = \frac{T\,T^* - T_0}{T^*\,T - T_0}\,T_0 \leq T \leq T^* \quad (20)$$

At temperatures above T^*, cooperative and noncooperative movements merge together[24] and Z is 1; below T^*, the relaxation times of cooperative movements can be obtained from the empirical Vogel–Fulcher–Tammann equation. This temperature T^* is of the order of $1.3T_g$ in polymers that are completely amorphous, and in semicrystalline polymers, T^* is equal to the melting temperature.[24] T_0 is a temperature below the glass-transition temperature (T_g) at which Z approaches infinity and $\tau_{\text{cooperative}}$ extrapolates to infinity. In the case of PEN, the α relaxation is associated with the cooperative motions, which reflect the dielectric manifestation of the glass transition, and the β^* relaxation has been associated with partially cooperative movements.

Figure 8 is a representation of the temperature dependence of the relaxation times of a polymeric system with three kinds of molecular motions: cooperative motions (α), partially cooperative motions (β^*), and noncooperative motions (β).

To obtain the isochronal diagrams of ε_r' and ε_r'' from eqs. (16) and (17), the cooperative (α) and partially cooperative (β^*) motions have been defined by eq. (19); eq. (18) has been used for noncooperative (β) movements.

Testing the response of the fractional model under isochronal conditions

To verify the dielectric behavior of the model defined by eqs. (15)–(17), we proceeded to vary systematically the fractional order of the cap resistors that constitute the DFM. These parameters can take values only between 0 and 1.

Figure 9 shows the isochronal predictions of ε_r' and ε_r'' at different values of b, with a, c, and d remaining constant.

In Figure 9, the $\varepsilon_r''(T)$ plot shows, per our fractional model prediction, the existence of three peaks corresponding to α, β^*, and β dielectric relaxations. The peak at lower temperatures corresponds to the β re-

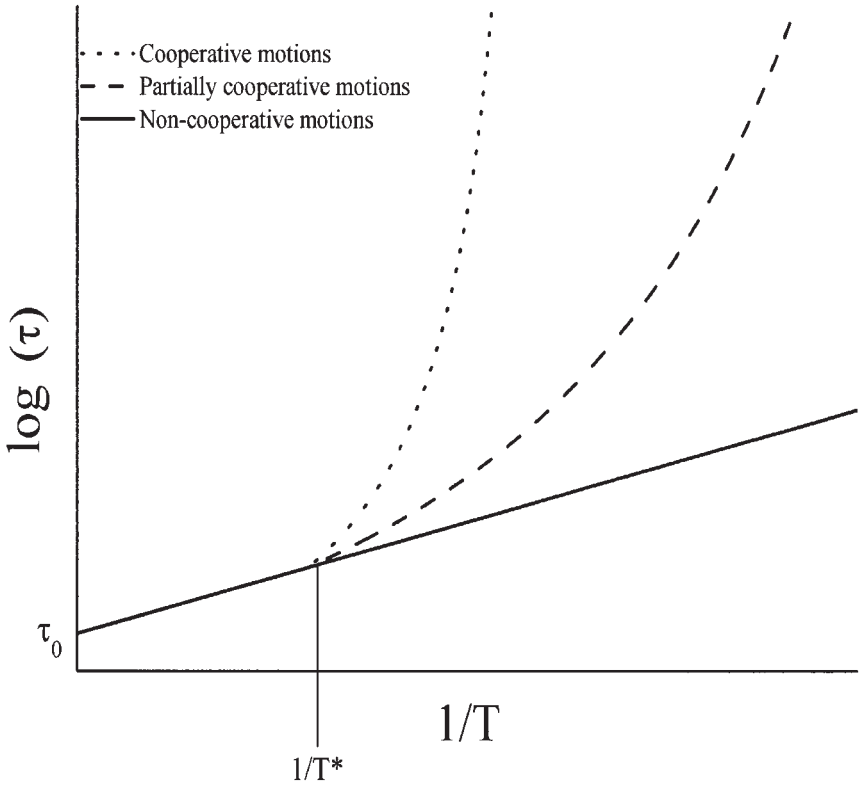

Figure 8 τ values of the different molecular motions of semicrystalline polymers.

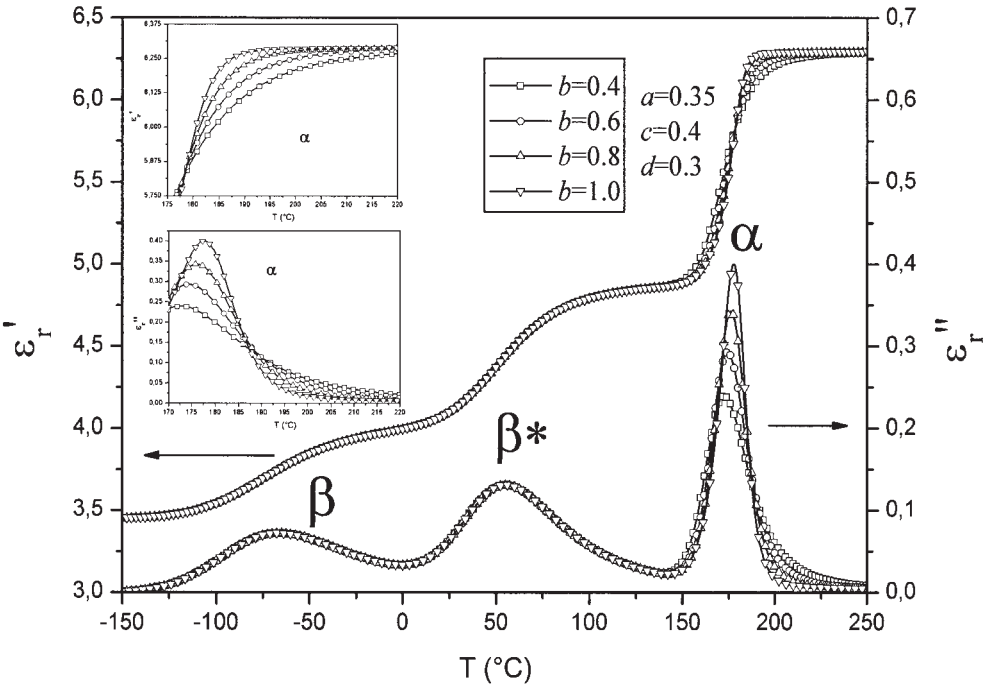

Figure 9 ε'_r and ε''_r under isochronal conditions at a frequency of 10 Hz. The parameters for α relaxation are $\varepsilon 1_{rs} = 2.5$, $\varepsilon 1_{r\infty} = 1.1$, $E_{a\ \text{elementary movement}} = 0.7$ eV, $\tau_b(T) = \tau_a(T)$, $\tau_0 = 1 \times 10^{-14}$ s, $T^* = 540$ K, and $T_0 = 350$ K. The parameters for β^* relaxation are $\varepsilon 2_{rs} = 2$, $\varepsilon 2_{r\infty} = 1.15$, $E_{a\ \text{elementary movement}} = 0.55$ eV, $\tau_0 = 1 \times 10^{-14}$ s, $T^* = 540$ K, and $T_0 = 150$ K. The parameters for β relaxation are $\varepsilon 3_{rs} = 1.8$, $\varepsilon 3_{r\infty} = 1.2$, $E_a = 0.5$ eV, and $\tau_0 = 1 \times 10^{-14}$ s.

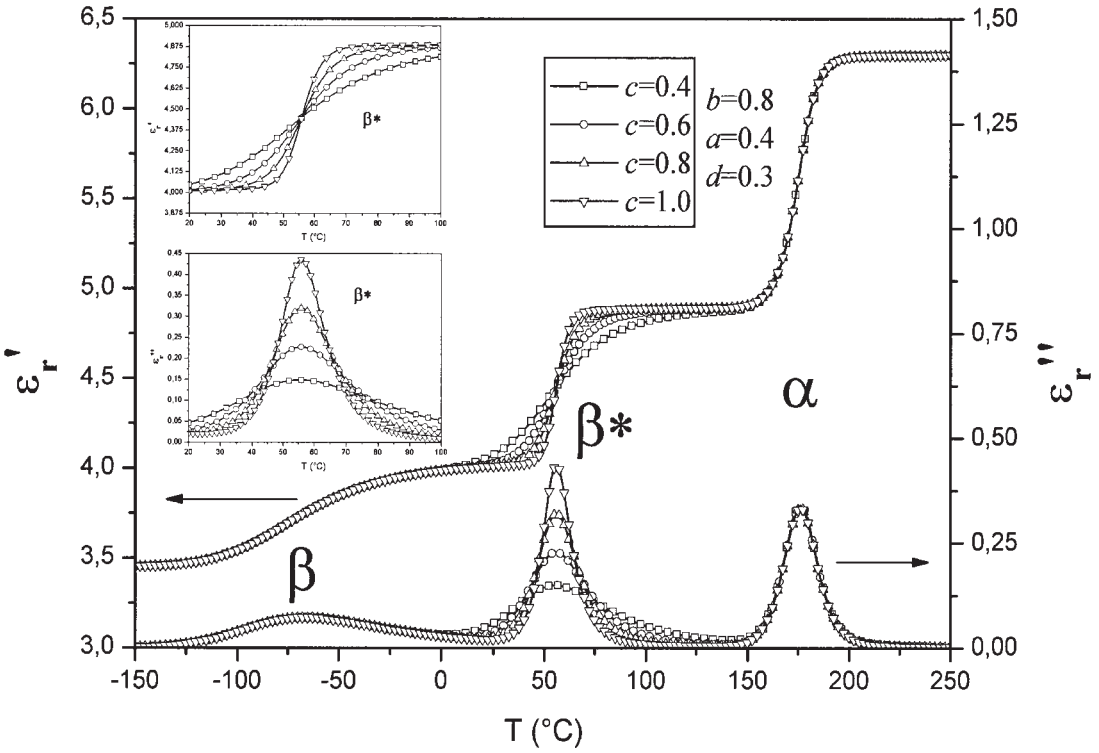

Figure 10 Isochronal predictions of ε_r' and ε_r'' with different values of c at a frequency of 10 Hz. The other DFM parameters correspond to Figure 9.

laxation, the second peak is associated with the β^* relaxation, and the last one at higher temperatures is related to the α relaxation. The maximum at the α relaxation increases as b increases. The shape of the curves of ε_r' and ε_r'' at the start of the α relaxation when the temperature decreases is strongly dependent on parameter b, whereas at the end of the curves parameter a determines the changes in ε_r' and ε_r''. Parameter a could also be associated with the zone placed between the α and β^* relaxations; this zone includes the minimum.

The effect of parameter c on ε_r' and ε_r'' is shown in Figure 10, the rest of the parameters remaining constant.

At higher values of c, the slope of the ε_r' curve is more pronounced, being practically vertical at values of c close to 1. On the other hand, the maximum of ε_r'' corresponding to the β^* relaxation increases when c increases. This parameter thus affects, on the one hand, the maximum of the β^* relaxation and, on the other hand, both the minima, one located between the α and β^* relaxations and other between β^* and β. Both these minima increase when c decreases.

Finally, Figure 11 shows the effect of parameter d on ε_r' and ε_r'', with a, b, and c remaining constant. The shape of ε_r' and ε_r'' in the region corresponding to the β relaxation is dependent on d. When parameter d increases, the maximum associated with the β relaxation also increases. On the other hand, d also affects the minimum located between the β^* and β relaxations; this minimum increases when d decreases.

We can deduce from Figures 9–11 the combined effect of parameters a and c in the region between the α and β^* relaxations and the combined effect of parameters c and d in the region between the β^* and β relaxations.

From the individual contributions of our DFM elements, we can make an approximation of the deconvolution of molecular movements and carry out a distinct analysis of each dielectric relaxation contribution on the global spectrum of the system. Figure 12 shows the global response of ε_r' and ε_r'' and the individual contributions of the model elements. The temperature dependence of ε_r' shows that at very low temperatures, ε_r' is equal to the global nonrelaxed permittivity ($\varepsilon_{r\infty}$):

$$\varepsilon_{r\infty} = \varepsilon 1_{r\infty} + \varepsilon 2_{r\infty} + \varepsilon 3_{r\infty} \tag{21}$$

On the other hand, at higher temperatures, ε_r' is equal to the global relaxed permittivity (ε_{rs}):

$$\varepsilon_{rs} = \varepsilon 1_{rs} + \varepsilon 2_{rs} + \varepsilon 3_{rs} \tag{22}$$

Figure 13 shows the Cole–Cole diagram for each element in our model; the figure also shows how to

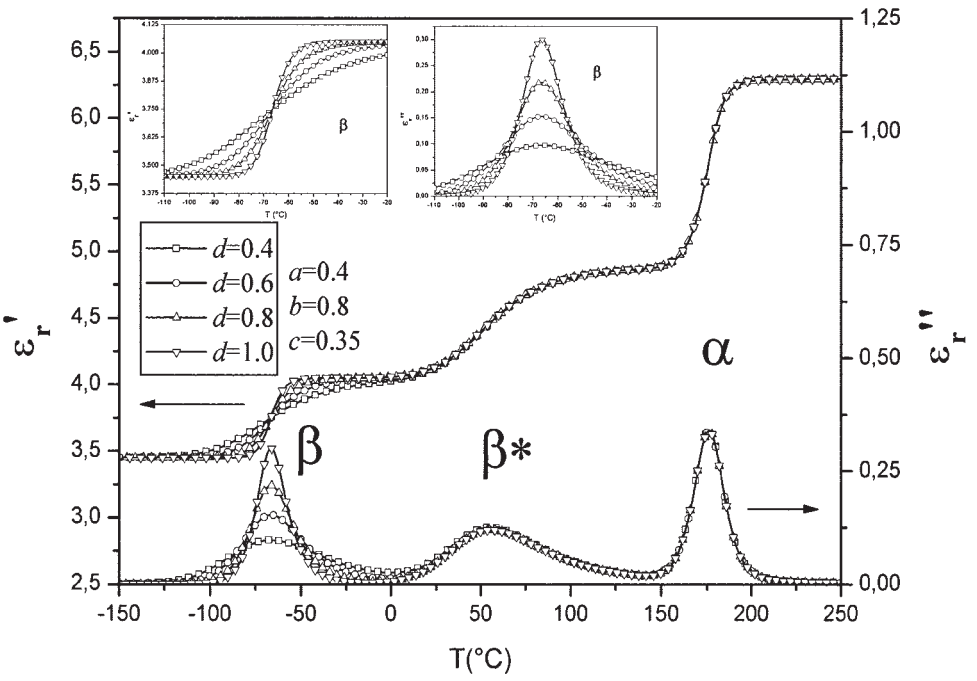

Figure 11 ε_r' and ε_r'' under isochronal conditions for different values of parameter d at a frequency of 10 Hz. The values of the remaining parameters correspond to Figure 9

calculate the parameters a, b, c, d, $\varepsilon 1_{rs}$, $\varepsilon 1_{r\infty}$, $\varepsilon 2_{rs}$, $\varepsilon 2_{r\infty}$, $\varepsilon 3_{rs}$, and $\varepsilon 3_{r\infty}$ from individual Cole–Cole diagrams.

In the next section, we compare the theoretical predictions of our DFM with experimental results of ε_r^* for a 45-μm-thick semicrystalline specimen of PEN with a crystallinity rate of 43%. Gold metallization was carried out on both sides of the sample to guarantee better contact with the electrodes of the dielectric analyzer used (DEA2979, TA Instruments, New Castle, DE).

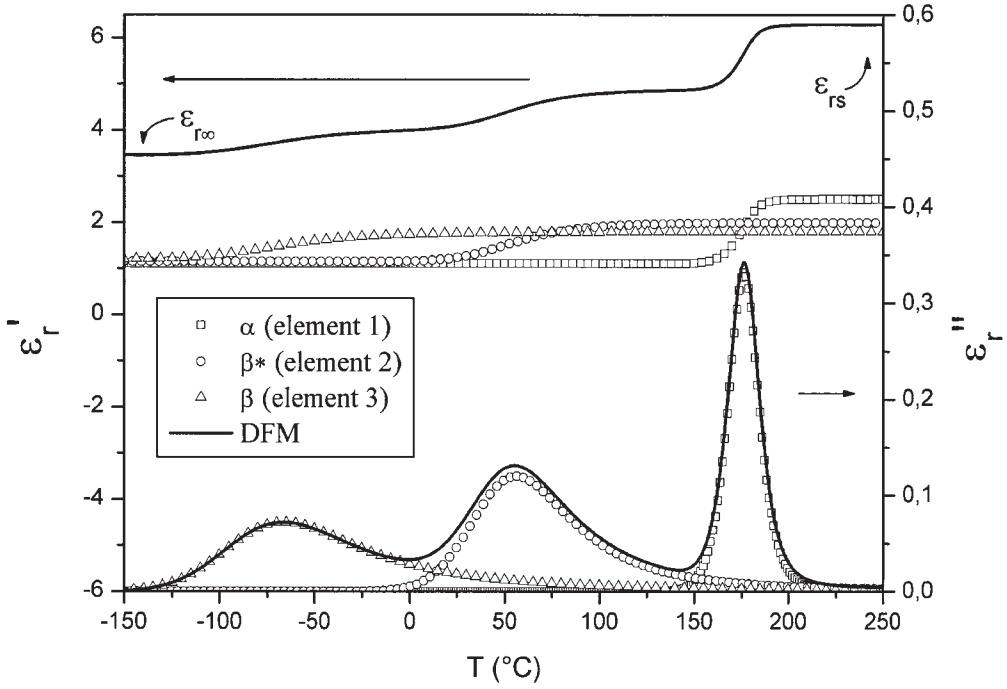

Figure 12 Individual contributions of each DFM element at f = 10 Hz, with a = 0.8, b = 0.4, c = 0.35, and d = 0.2. The activation parameters are those of Figure 9.

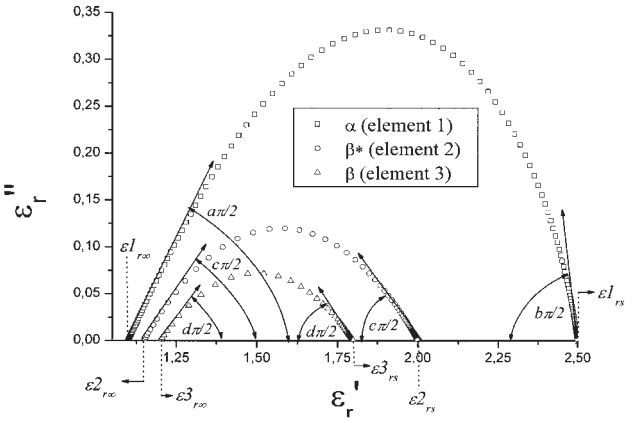

Figure 13 Cole–Cole diagrams for each element of the model based on individual contributions, corresponding to Figure 12.

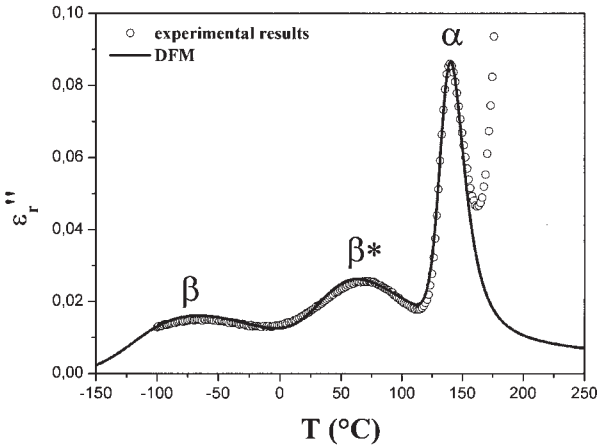

Figure 15 Comparison of the model predictions and experimental data for $\varepsilon''_r(T)$ at 10 Hz.

COMPARISON OF THE EXPERIMENTAL RESULTS AND DFM PREDICTIONS

Figures 14–16 show a good agreement between the model predictions and experimental results obtained for ε'_r and ε''_r at a frequency of 10 Hz from 100 to 160°C.

In Figure 14, each relaxation mode is manifested by an increase in ε'_r with increasing temperature. They are also associated with three ε''_r peaks (Fig. 15).

At $T > 160$°C, the imaginary part of the complex permittivity increases with an increase in temperature, and this behavior is associated with the phenomenon of conductivity and is not predicted by our DFM. With a frequency set at 10 Hz, the α relaxation is found at $T \approx 140$°C, β^* is found at $T \approx 70$°C, and β is found at $T \approx -66$°C.

Table I shows the values of the DFM parameters used to obtain the predictions of ε'_r and ε''_r in Figures 14–16. The fractional orders of the cap resistors show the next behavior: $b > a > c > d$. As a first approximation, molecular motions related to the β relaxation can be represented by parameter d, the partially cooperative motions related to the β^* relaxation can be represented by parameter c, and parameters a and b could be used to represent cooperative motions related to the α relaxation.

The molecular motions associated with the dielectric manifestation of α are cooperative movements within the temperature range of $T_0 \approx T_g - 50$°C to $T^* \approx 267$°C. In this case, T^* is equal to the melting point of PEN. From eqs. (19) and (20), we can estimate the apparent activation energy (E_{apparent}) of the α-cooperative motions from the next equation:

$$E_{\text{apparent}} = (E_{\text{a elementary movements}})(Z) = (E_{\text{a elementary movements}}) \times \left(\frac{T\,T^* - T_0}{T^*\,T - T_0}\right) \quad (23)$$

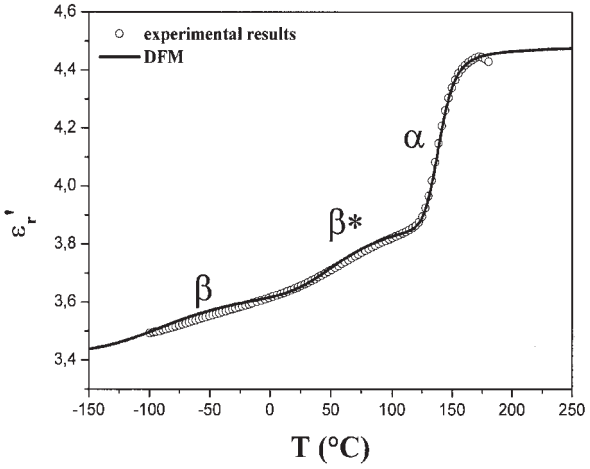

Figure 14 Comparison of the model predictions and experimental data for $\varepsilon'_r(T)$ at 10 Hz.

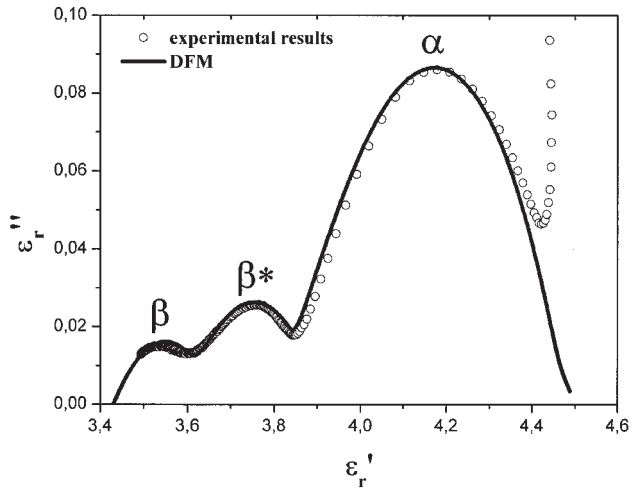

Figure 16 Comparison of the model predictions and experimental data for Cole–Cole diagrams at 10 Hz.

TABLE I
Parameters of the DFM

α relaxation: Cooperative motions		β^* relaxation: Partially cooperative motions			β-relaxation: Noncooperative motions	
b^-	0.41	c	0.19		d	0.17
a	0.24					
$(\varepsilon 1_{rs} - \varepsilon 1_{r\infty})$	0.58	$(\varepsilon 2_{rs} - \varepsilon 2_{r\infty})$	0.25		$(\varepsilon 3_{rs} - \varepsilon 3_{r\infty})$	0.24
$E_{a\text{elementary movements}}$	0.47eV	$E_{a\text{elementary movements}}$	0.56		E_{apparent}	0.5
τ_0	1×10^{-14} s	τ_0	1	$\times 10^{-14}$s		
T^*	540 K (267°C)	T^*	540K (267°C)		τ_0	1×10^{-14}s
T_0	349 K (76°C)	T_0	190K (−83°C)			

For β^*, the molecular motions are less cooperative than α movements; T^* in this case is also equal to the melting point of PEN, and T_0 is less than $T_g - 50$°C. E_{apparent} of the β^* partially cooperative movements is also defined by eq. (23) with the corresponding activation parameters shown in Table I.

For the β relaxation, E_{apparent} has a low value corresponding to noncooperative processes. Figure 17 shows E_{apparent} for α, β^*, and β processes obtained from activation parameters shown in Table I.

CONCLUSIONS

The method of derivation and fractional integration has enabled us to develop a model that accounts for the dielectric behavior of polymers with three distinct relaxation phenomena.

Choosing arbitrarily the values of the fractional orders of cap resistors in our fractional model, we have calculated for an applied sinusoidal form ε_r' and ε_r''. These diagrams have enabled us to analyze the effects of the model parameters on the α, β^*, and β dielectric relaxations. The parameters a and b are mainly associated with the α relaxation, parameter c is associated with β^*, and parameter d is associated with β.

The transition zones between the α and β^* relaxations and the β^* and β relaxations are associated with parameters a and c and parameters c and d respectively. These transition zones are very important because they are very sensitive to the phenomena of physical aging.[9]

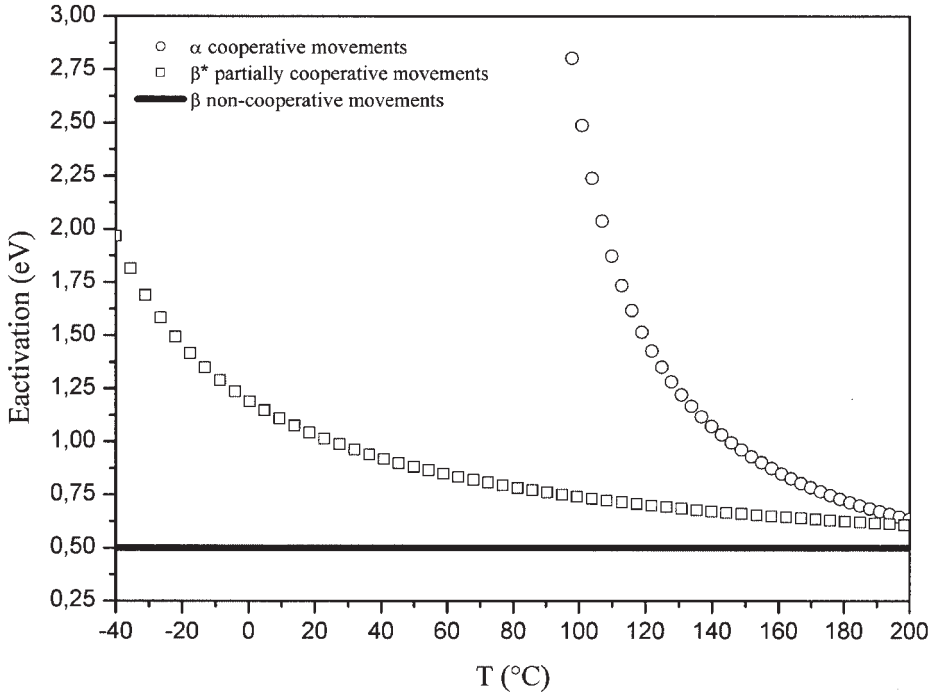

Figure 17 E_{apparent} for the α, β^*, and β processes.

The comparison between the experimental results and DFM predictions has enabled a molecular interpretation of our DFM parameters. In the continuation of our work, we will analyze the experimental measurements of ε_r^* for PEN specimens at different crystallinity rates. This will enable us to improve the molecular interpretation of our DFM parameters.

References

1. Novikov, V. U.; Kozlov, G. V. Russ Chem Rev 2000, 69, 572.
2. Guerrero, C.; Reyes, E.; Gonzalez, V. Polymer 2002, 43, 6683.
3. Gonzalez, V. A.; Alanis, M.; Guerrero, C.; Ortiz, U. J Polym Sci Part B: Polym Phys 2004, 42, 646.
4. Carpinteri, A.; Cornetti, P. Chaos Solitons Fractals 2002, 13, 85.
5. Nigmatullin, R. R.; Osokin, S. I.; Smith, G. J Phys: Condens Matter 2003, 15, 3481.
6. Butzer, P. L.; Westphal, U. In Applications of Fractional Calculus in Physics; Hilfer, R., Ed.; World Scientific: River Edge, NJ, 2000; p 1.
7. Bagley, R. L.; Torvik, P. J. J Rheol 1986, 30, 133.
8. Schiessel, H.; Blumen, A. J Phys A: Math Gen 1993; 26, 5057.
9. Alcoutlabi, M.; Martinez-Vega, J. J. Polymer 2003, 44, 7199.
10. Heymans, N. Signal Process 2003, 83, 2345.
11. Moshrefi-Torbati, M.; Hammond, J. K. J Franklin Inst B 1998, 335, 1077.
12. Reyes-Melo, E.; Martinez-Vega, J.; Guerrero-Salazar, C.; Ortiz-Mendez, U. Revue des Composites et de Matériaux Avancés; Hermes Science: Paris, 2002; Vol. 12, No. 2.
13. Reyes-Melo, M. E.; Martinez-Vega, J. J.; Guerrero-Salazar, C.; Ortiz-Mendez, U. Presented at the Colloque sur les Matériaux du Génie Electrique, Grenoble, France, April 2, 2003.
14. Reyes-Melo, E.; Martinez-Vega, J.; Guerrero-Salazar, C.; Ortiz-Mendez, U. J Appl Polym Sci 2004, 94, 657.
15. Reyes-Melo, M. E.; Martinez-Vega, J. J.; Salvia, M. Presented at the Colloque Electrotechnique du Futur, Supélec, Gif-sur-Yvette, Paris, France, Dec 9, 2003.
16. Mayoux, C.; Martinez-Vega, J. J.; Guatavino, J.; Laurent, C. IEEE Trans Dielectr Electr Insulation 2001, 8, 58.
17. Martinez-Vega, J. J.; Zouzou, N.; Boudou, L.; Guastavino, J. IEEE Trans Dielectr Electr Insulation 2001, 8, 776.
18. Zouzou, N. Thesis, Universite Paul Sabatier, 2002.
19. Hardy, L.; Stevenson, I.; Fritz, A.; Boiteux, G.; Seytre, G.; Schönhals, A. Polymer 2003, 44, 4311.
20. Alcoutlabi, M.; Martinez-Vega, J. J. Polymer 1998, 39, 6269.
21. Alegria, A.; Guerrica-Echevarria, E.; Telleria, I.; Colmenero, Journal Physical Review B 1993, 47, 14857.
22. Ezquerra, T. A.; Liu, F.; Boyd, R. H. Polymer 1997, 38, 5793.
23. Matsuoka, S. J Res Natl Inst Stand Technol 1997, 102, 213.
24. Rault, J. J Non-Cryst Solids 2000, 271, 177.
25. Ngai, K. L. J Chem Phys 1998, 109, 6982.